は，同部位に明らかなθ帯域の活動を認めなかったと報告している．一方，Ropohlら[16]は幻聴を有する33歳の男性統合失調症患者と13人の正常対照者を対象として自発MEGを測定し，統合失調症患者群の左聴覚野において，12.5Hzから30Hzの速波成分の増加を認めたが，正常対照者群では認めなかったと報告している．

2．聴覚関連以外のMEG研究

まず，視覚誘発MEGに関する所見を紹介する．Streitら[17]は15人の統合失調症患者と12人の正常対照者を対象として表情認知時のMEGを記録し，統合失調症患者群においては正常対照者群と比較して，表情認知の際に下部前頭前野，後頭葉，側頭葉，下部頭頂葉の活動が低下していることを報告した．また，Löwら[18]は10人の統合失調症患者と10人の正常対照者を対象として，提示した写真をカテゴリー分けする課題を遂行する際のMEGを記録し，統合失調症患者群においては視覚野からの腹側経路(visual ventral processing stream)に関連していると思われる両側頭部領域の機能低下を認め，またこの機能低下の程度が陰性症状と関連していたと報告している．

次に，体性感覚誘発MEGに関する所見を紹介する．Reiteら[19]は14人の統合失調症患者と15人の正常対照者において，手指へ触覚刺激を与えた際のMEGを記録し，得られたMEG波形におけるM50成分の一次感覚野内の等価電流双極子を推定したところ，統合失調症者群においては，正常対照者群と比べて等価電流双極子のベクトルの向きが反対で，位置が正常対照者よりも前下方にずれていたことを報告している．

Kawaguchiら[20]は，5人の幻聴を有しない統合失調症患者，4人の幻聴を有する統合失調症患者および6人の正常対照者を対象としてStroop課題遂行時のMEGを測定した．正常対照者では両側前頭前野背外側部に，とくに左側に優位な賦活を認めた．一方，幻聴を有しない統合失調症患者では左前頭前野背外側部の賦活を認め，幻聴を有する統合失調症患者では右前頭前野背外側部の賦活を認めた．彼らはこれらの結果から，幻聴が左前頭前野背外側部の機能異常と関連するのではないかと考察している．さらに，彼らは統合失調症患者群において，正常対象者群と同様に下頭頂領域・中側頭領域－前頭前野背外側部－運動野の順に神経活動を認めたと報告し，基本的な情報処理機構は保持されていると考えた．

おわりに

MEGの原理および解析方法，統合失調症におけるMEG研究を聴覚に関するものを中心に紹介した．今後MEGが，その比較的高い空間分解能と時間分解能により，統合失調症の病態解明に寄与していくことが期待される．

文　献

1) 太田克也．脳磁図．臨床精神医学 2004；33 Suppl：589-95.
2) 柿木隆介，渡辺昌子，三木研作．脳磁図(MEG)．臨床検査 2005；49：1557-62.
3) 篠崎和弘，鵜飼　聡，石井良平，ほか．精神分裂病のMEG研究．精神科治療学 2001；16：1055-61.
4) 松岡洋夫，中村真樹．統合失調症の認知障害と脳波．精神経誌 2005；107：307-22.
5) Thoma RJ, Hanlon FM, Moses SN, et al. Lateralization of auditory sensory gating and neuropsychological dysfunction in schizophrenia. Am J Psychiatry 2003 ; 160 : 1595-605.
6) Edgar JC, Miller GA, Moses SN, et al. Cross-modal generality of gating deficit. Psychophysiology 2005 ; 42 ; 318-27.
7) Thoma RJ, Hanlon FM, Moses SN, et al. M50 sensory gating predicts negative symptoms in schizophrenia. Schizophr Res 2005 ; 73 : 311-8.
8) Näätänen R, Gaillard AW, Mantysalo S. Early selective-attention effect on evoked potential reinterpreted. Acta Psychol 1978 ; 42 : 313-29.
9) 斎藤　治，豊島良一．事象関連電位；歴史と概論．In：丹羽真一，鶴　紀子・編．事象関連電位－事象関連電位と神経情報科学の発展－．東京：新興医学出版社；1997. p. 3-21.
10) Shelley AM, Ward PB, Catts PT, et al. Mismatch negativity : an index of a preattentive processing deficit in schizophrenia. Biol Psychiatry 1991 ; 30 : 1059-62.
11) Kasai K, Yamada H, Kamio S, et al. Neuromagnetic

correlates of impaired automatic categorical perception of speech sounds in schizophrenia. Schizophr Res 2002 ; 59 : 159-72.

12) Kasai K, Yamada H, Kamio S, et al. Do high or low doses of anxiolytics and hypnotics affect mismatch negativity in schizophrenic subjects? An EEG and MEG study. Clin Neurophysiol 2002 ; 113 : 141-50.

13) Yamasue H, Yamada H, Yumoto M, et al. Abnormal association between reduced magnetic mismatch field to speech sounds and smaller left planum tempolare volume in schizophrenia. Neuroimage 2004 ; 22 : 720-7.

14) 笠井清登，山末英典，荒木　剛．統合失調症の画像・神経生理学的研究の展望．精神経誌2004；106：851-66.

15) Ishii R, Shinosaki K, Ikejiri Y, et al. Theta rhythm increases in left superior temporal cortex during auditory hallucinations in schizophrenia : a case report. Neuroreport 2000 ; 11 : 3283-7.

16) Ropohl A, Sperling W, Elstner S, et al. Cortical activity associated with auditory hallucinations. Neuroreport 2004 ; 15 : 523-6.

17) Streit M, Ioannides A, Sinnemann T, et al. Disturbed facial affect recognition in patients with schizophrenia associated with hypoactivity in distributed brain regions : A magnetoencephalographic study. Am J Psychiatry 2001 ; 158 : 1429-36.

18) Löw A, Rockstroh B, Elbert T, et al. Disordered semantic representation in schizophrenic temporal cortex revealed by neuromagnetic response patterns. BMC Psychiatry 2006 ; 6 : 23.

19) Reite M, Teale P, Rojas DC, et al. Anomalous somatosensory cortical localization in schizophrenia. Am J Psychiatry 2003 ; 160 : 2148-53.

20) Kawaguchi S, Ukai S, Shinosaki K, et al. Information processing flow and neural activations in the dorsolateral prefrontal cortex in the stroop task in schizophrenic patients. Neuropsychobiology 2005 ; 51 : 191-203.

*　　*　　*

特集2

リチウム薬理の多様性

リチウムの病相予防作用

大林長二（おおばやしちょうじ），鬼塚俊明（おにつかとしあき）
九州大学大学院医学研究院精神病態医学（〒812-8582 福岡市東区馬出3丁目1-1）
E-mail : choji77@npsych.med.kyushu-u.ac.jp

SUMMARY

双極性障害は再発頻度の高い疾患であり再発予防は治療上，重要な位置を占める．lithiumは最も歴史のある気分安定薬であり，躁病相，うつ病相に対する効果のみならず病相予防作用をも持つことが確認された唯一の薬剤である．双極性障害の継続期・維持期治療に関してAPA，Expert Consensus 2000といったガイドラインではlithiumをfirst-line治療薬として挙げている．lithiumは躁病相が誇大的・爽快なもの，家族歴に躁病を持つものや，循環性格の症例に有効であり，病相構造からみると躁病相→うつ病相→間欠期を呈するケースの病相予防に有効である．他の気分安定薬との併用療法も有効であるが，lithiumの効果が乏しい症例もみられる．今後，日本未発売薬剤の発売などにより病相予防可能なケースが増えることが期待される．

KEY WORDS
リチウム
気分安定薬
双極性障害
予防
維持療法

はじめに

双極性障害は再発頻度の高い疾患であり再発予防は治療上，重要な位置を占める．1954年，Schouら[1]が双極I型障害に対するlithiumの短期治療および予防的効果について臨床的知見を示した．現在なお双極性障害の治療においてlithium，valproic acid，carbamazepineといった気分安定薬は薬物療法の中心であり，なかでもlithiumは，躁病エピソード，うつ病エピソードに対する効果のみならず病相予防作用を持つことが確認された唯一の薬剤である[2]．本稿では双極性障害の継続期・維持期治療のガイドラインにふれ，lithiumの病相予防作用についてvalproic acid，carbamazepine等との比較を通して述べることとする．

I. 継続期・維持期治療のガイドラインについて

双極性障害は，躁病エピソードとうつ病エピソードを繰り返す特徴があり，Silverstoneら[3]は，発病後5年以内に2～3回のエピソードの再発がみられると報告している．Gitlinら[4]は，82人の双極性障害を平均4.3年追跡調査し，5年間の躁転・うつ転率を73％と推定した．このように双極性障害は再発率が高く，その治療は，一般に急性期治療，回復期治療（継続療法）に引き続き，長期再発予防治療（維持療法）へと移行す

1344-0128/06/¥100/頁/JCLS

る．ここで継続療法・維持療法という用語について述べておく．継続療法とはエピソードが完全に終了する前に消えかけていた症状が再燃することを防ぐ治療のことであり，急性期症状消失からある一定期間行われるものである．維持療法とはエピソードが完全に終了した後，新たにエピソードが始まる（再発）を防ぐ治療のことであり，エピソードが完全に終了した後に開始されるものである．継続期・維持期治療に関して，**表1**に示すようにほとんどのガイドラインが，双極I型障害の患者のうち2回以上の躁病エピソード，あるいは1回の重症躁病エピソードと双極性障害の家族歴を持つ者に長期再発予防治療を推奨している．継続療法から維持療法へ移行するか否かについてAPA[5]によれば『維持療法を開始するか否かは，維持的薬物療法の有無による再発の頻度の相違や，その治療に伴う危険性と負担などに関する判断に基づいて決定される．その決定は，患者，精神科医そして可能ならば家族の参加を得てなされるべきである．その際，少なくとも2年間は予防療法を継続することにおいて医師－患者間で同意が得られていることが望ましい』とされている．双極性障害の治療に有効な薬物には，気分安定薬（lithium，valproic acid，carbamazepine）の他にも定型抗精神病薬（haloperidol，zotepine，sultopride），非定型抗精神病薬（risperidone，olanzapine，quetiapine，aripiprazole），抗うつ薬（fluvoxamine，fluoxetine［日本未発売］，paroxetine，sertraline）等がある．久住ら[10]は，病相予防効果の期待される薬剤としてlamotrigine（日本未発売），topipramate（日本未発売），gabapentin，oxcarbazepine（日本未発売），zonisamide，phenytoinといった抗てんかん薬も挙げている．いずれかの薬物を選択し急性期を経過したとして，継続期・維持期において再燃・再発しないよう，如何にして薬物療法を行ってゆくかは日常診療において難渋するところである．渡邉[11]は『①過去の病相経過，②過去の急性期治療で寛解が得られたか否か，③身体的合併症や依存薬物の有無（アルコールを含む），④環境要因・ストレス情況など』といった点に注意して維持療法期の処方を変更するべきとしている．さらに，渡邉[11]は『躁病相の維持療法下では，躁病治療に用いられている抗精神病薬を徐々に減量して，気分安定薬のみの処方にする努力が必要であろう．またうつ病相の維持療法でも抗うつ薬を減量し，気分安定薬のみの処方にできれば理想的である．』と述べている．維持療法下では，抗精神病薬，抗うつ薬の減量をすすめ，気分安定薬のみの処方とすることが目標であろう．現在，気分安定薬と非定型抗精神病薬の併用療法がスタンダードになってきているが，安易な多剤併用療法は避け，気分安定薬を中心とした処方とし，薬剤のスリム化への努力は必要であると考える．

II. lithium, valproic acid, carbamazepineにおける病相予防効果の比較

1. lithium

1）再発率

Bauerら[12]は，気分安定薬とは，急性の躁症状の改善，急性のうつ症状の改善，躁病相およびうつ病相の予防といった効果を有するものと定義している．lithiumは最も歴史のある気分安定薬であり，躁病エピソード，うつ病エピソードに対する効果のみならず病相予防作用も持つことが確認された唯一の薬剤である．**表1**に示すように継続期・維持期治療のfirst-line治療として気分安定薬を挙げるものは多く，中でもAPA[5]，Expert Consensus 2000[6]はlithiumをfirst-line治療薬として挙げている．Solomonら[13]によれば，病相予防効果をlithium服用群とプラセボ服用群とで比較すると，再発率はlithium服用群で0～44％，プラセボ服用群では38～93％であったという．また，Davisら[14]によればlithium服用群では29％，プラセボ服用群では74％であったと述べている．Geddesら[15]は，躁病エピソードの再発率はlithium服用群で14％，プラセボ服用群で24％であり，うつ病エピソードの再発率はlithium服用群で25％，プラセボ服用群で32％であったと報告した．Baldessariniら[16]は，1970～1990年代に発表されたlithiumの長期投与試験に関する報告24報を年代ごとに比較した結果，lithium治療中の患者の再発率は30年間減少傾向にあること，lithiumによる治療を受けていない患者の再発率はlithiumによる治療を受けている患者の約19倍であり，そのリスクは30年間変わっていなかったことを報告した．

表1　双極性障害の継続期・維持期治療

ガイドライン	first-line 治療	second-line 治療	継続期・維持期治療開始の目安
APA[5]	lithium	divalproex 又は carbamazepine	長期治療は患者の個人的リスク／ベネフィット比による
Expert Consensus 2000[6]	lithium 又は divalproex	carbamazepine	躁病相2回，重度躁病相1回，軽躁病相（双極II型）3回と抗うつ薬惹起性軽躁病の場合，生涯の予防投与を行う
VA[7]	推奨されている薬剤と期間は特定できていない		抗精神病薬またはbenzodiazepineの漸減 心理社会的リハビリテーションを強化
TMAP[8]	推奨薬剤はない		躁病相2回，家族歴をもつ躁病相1回の場合，生涯の予防投与を行う 最低の治療至適血中濃度となるような用量

APA : American Psychiatric Association, VA : Clinical practice guidelines for bipolar disorder from the Department of Veterans Affairs, TMAP : Texas Medication Algorithm Project
（文献[9]の表を改変して作成）

2）有効な臨床上の特徴

前述のようにlithiumの病相予防効果は明らかであるが，一方でRybakowskiら[17]の10年転帰をみた研究において，lithium単剤で病相が完全に予防されるのはわずかに1/4～1/3の症例に過ぎないと報告されている．また，lithiumはrapid cycler（急速交代型）には効果が乏しいことも知られている．どういった病像がlithiumに反応するのであろうか．**表2**に気分安定薬に反応する臨床指標[18]を示す．躁病相が誇大的・爽快なもの，あるいは家族歴に躁病を持つものや，性格が循環性格であるものにlithiumが有効と考えられている．逆に，精神病像を伴う躁病，急性交代型，躁・うつ混合状態を呈するもの，アルコール依存症を伴うもの，性格が内向的・神経症であるもの，さらに，発症年齢が若い症例はlithiumの反応が乏しいとされている．また，双極性障害におけるlithium選択の指針として，どのような病相経過をとるかということも重要である．岸本[19]は病相経過を構成する指標として，①病相頻度，②躁・うつ循環の有無とその順序，③躁病相/うつ病相比とそれらの重症度，④間欠期の有無の4項目を挙げ，それらを総合して病相構造とよんだ．この病相構造におけるlithiumの反応性をKukopulosら[20]は検討している．lithium予防投与に最もよく反応するものは，躁病相→うつ病相→間欠期という病相経過を呈するケースであり，とりわけ，軽躁病相→うつ病相→間欠期という経過型は極めてよく反応すると指摘している．逆にlithiumへの反応性が低かったのは，躁病相とうつ病相が間欠期を持たずに頻繁に繰り返される持続循環経過－短周期のものであったという．他に，うつ病相→躁病相→間欠期の病相経過を呈するケースでも反応性は低いといわれている．

3）投与基準と抗自殺効果

lithiumの具体的な投与量について，池田ら[21]は事前に腎機能の確認を行った後，初期投与量は，年齢，体格や病態により200～800 mgとするとし，約1週間でlithium血中濃度が平衡状態に達するため，この時点で血中濃度を測定するよう述べている．Gelenbergら[22]は維持療法期におけるlithium血中濃度に関して，低

表2　気分安定薬に反応する臨床指標

	lithium	valproic acid	carbamazepine
適応指標	爽快多幸気分 誇大妄想 循環性格 躁病の家族歴がある 軽症躁状態 （双極II型）	急速交代型 混合型 過去の病相回数が多い 脳波上非突発性異常波 頭部外傷の既往	急速交代型 混合型 精神病像を伴う躁病 分裂感情障害 不機嫌の傾向が強い 重症躁状態 気分障害の家族歴がない 発症年齢が若い
不適応指標	精神病像を伴う躁病 急速交代型 混合型 内向的・神経症性格 アルコール依存症 発症年齢が若い 甲状腺機能低下症 腎機能障害 妊婦	高アンモニア血症 肝機能障害	うつ病相が長いもの 貧血，白血球減少症 免疫機能の低下しているもの

（文献[18]の表を一部改変して作成）

血中濃度群（0.4 ～ 0.6 mEq/l，平均 0.54 mEq/l）と標準血中濃度群（0.8 ～ 1.0 mEq/l，平均 0.83 mEq/l）を比較した．低血中濃度群では 38 %が再燃するが，標準血中濃度群では 13 %と再燃率は低く，低血中濃度群は再発リスクは 2.6 倍高いものの手指振戦や口渇などの副作用は標準血中濃度群で高かったと報告している．APA[5]によると，維持療法期の lithium の至適濃度は 0.6 ～ 0.8 mEq/l とされている．双極性障害患者の自殺率は非常に高く，19 %[2]，15 %[23]ともいわれているが，Muller-Oerlinghausen ら[24]は lithium 投与群の自殺率は，非投与群と比較して 1/8 であったと報告しており，lithium には自殺率を低下させる効果があると述べている．また，Tondo ら[25]は lithium 投与群では lithium 非投与群と比較して，自殺のリスクは 82 %減少していたと報告した．Shastry ら[23]も lithium の抗自殺効果について報告しており，lithium が優れた自殺予防効果を持つとする報告は多い．一方で，lithium による維持療法を少なくとも 2 年間続け寛解状態が維持された後，lithium 中止の決断をすることは苦慮するところである．lithium の急激な中止後，早期に躁病エピソードが離脱的に誘発されやすいことが知られており[26]，lithium を中断する場合には数ヵ月かけて徐々に減量することが推奨されている[5]．

2. 他の気分安定薬（valproic acid, carbamazepine）との比較

lithium 以外にも日常臨床でよく使われている気分安定薬として valproic acid と carbamazepine がある．次に，それらが有効と思われる臨床指標と病相予防作用について lithium と比較して述べることとする．

1）valproic acid

表2 に示すように，valproic acid は急速交代型の症例，抑うつ症状を伴うような混合型病像，過去の病相回数が多い症例，脳波上非突発性異常波が存在する症例および頭部外傷の既往のある症例には lithium より valproic acid の方が有効といわれている．双極性障害の継続期・維持期治療では，**表1** に示すように APA[5]において second-line 治療薬，Expert Consensus 2000[6]においては first-line 治療薬として valproic acid が挙げられている．病相予防作用については，Bowden ら[27]の

躁病エピソードから回復した双極I型障害患者に対する12ヵ月間のlithium，valproic acid，プラセボの比較試験の報告がある．それによると，躁病またはうつ病エピソードの再発までの期間はlithium服用群，valproic acid服用群，プラセボ服用群の3群間で有意差はなかった．しかし，valproic acid服用群は，プラセボ服用群より再発に伴う治療中断例が少なく，lithium服用群より維持療法を続けられる期間が長く，抑うつ症状の悪化は少なかったという．Solomonら[28]はithiumによる維持療法中の患者にvalproic acidあるいはプラセボを追加して1年間経過をみたところvalproic acid併用群の方が有意に再発が少なかったと報告している．valproic acidもlithium同様病相予防に有効であり，lithium単剤療法より併用療法の方がより効果が高いと言えるかも知れない．

2）carbamazepine

表2に示すように，carbamazepineは急速交代型の症例，精神病像を伴う症例，混合型病像を持つ症例，重症躁状態の症例，気分障害の家族歴がない症例および発症年齢が若い症例などに対し，lithiumより有効性が高いといわれている．双極性障害の継続期・維持期治療において**表1**に示すようにAPA[5]，Expert Consensus 2000[6]いずれにおいてもsecond-line治療薬としてcarbamazepineは挙げられている．病相予防作用について，Denicoffら[29]の維持療法期におけるlithiumとcarbamazepineとの比較報告がある．それによると，lithiumの有効率は33.3％，carbamazepineの有効率は31.4％であったが，lithium，carbamazepine併用では55.2％であったという．Hartongら[30]の維持療法期におけるlithiumとcarbamazepineとの比較において再発患者はlithium服用群44例中12例（27.2％），carbamazepine服用群50例中21例（35.6％）であった．carbamazepineよりlithiumの方が病相予防に有効であり，lithium単剤療法より併用療法の方がより効果が高い可能性がある．

おわりに

双極性障害の継続期・維持期におけるlithiumの病相予防作用に関して，ガイドラインにふれ，予防効果の発揮されやすい臨床上の特徴を述べ，他の気分安定薬（valproic acid，carbamazepine）と比較した．現在なおlithiumは双極性障害の急性期のみならず，継続期・維持期における薬物療法の中心であるが，lithiumはすべての症例に病相予防ができるわけではない．今後，lamotrigine等の本邦未発売の薬剤が発売されることで選択肢が増え，同時に守備範囲も広がり，一人でも多くの患者の病相が予防されることを期待してやまない．

参考文献

1) Schou M, et al : The treatment of manic psychoses by the administration of lithium salts. J Neurol Neurosurg Psychiatry **17** : 250, 1954.
2) Goodwin FK, et al : Manic-Depressive Illness. Oxford University Press, New York, 1990.
3) Silvesterstone T, et al : Long term treatment of bipolar disorder. Drugs **51** : 367-382, 1996.
4) Gitlin MJ, et al : Relapse and impairment in bipolar disorder. Am J Psychiatry **152** : 1635-1640, 1995.
5) American Psychiatric Association : Practice guideline for the treatment of patients with bipolar disorder . Am J Psychiatry **151** (suppl.) : 1-36, 1994.
6) Sachs GS, et al : The Expert Consensus Guideline Series : Medication Treatment of Bipolar Disorder 2000. Postgrad Med (Apr ; Spec) : 1-104, 2000.
7) Bauer MS, et al : Clinical practice guidelines for bipolar disorder from the Department of Veterans Affairs. J Clin Psychiatry **60** : 9-21, 1999.
8) Dennehy EB, et al : Medication algorithms for bipolar disorder. J Pract Psychiatry Behav Health **5** : 142-152, 1999.
9) 大坪天平：治療計画（双極性障害）：外来治療．精神科治療学 **17**（増）：64-72, 2002.
10) 久住一郎，他：新たなムードスタビライザー（双極性うつ病－双極性障害の新たな治療ターゲット）．臨床精神薬理 **8** : 317-323, 2005.
11) 渡邊昌祐：双極性障害の急性期治療・維持療法・予防．精神科治療学 **17**（増）：103-115, 2002.
12) Bauer MS, et al : What is a "mood stabilizer" ? An evidence-based response. Am J Psychiatry **161** : 3-18, 2004.
13) Solomon DA, et al : Course of illness and maintenance treatments for patients with bipolar disorder. J Clin Psychiatry **56** : 5-13, 1995.
14) Davis JM, et al : Mood stabilizers in the prevention of recurrent affective disorders : A meta-analysis. Acta Psychiatr Scand **100** : 406-417, 1999.
15) Geddes JR, et al : Long-term lithium therapy for bipolar disorder : systematic review and mete-analysis of randomized controlled trials. Am J Psychiatry **161** : 217-222, 2004.

16) Baldessarini RJ, et al : Does lithium treatment still work? Arch Gen Psychiatry **57** : 187-190, 2000.
17) Rybakowski JK, et al : The prophylactic effect of long-term lithium administration in bipolar patients entering treatment in the 1970s and 1980s. Bipolar Disord **3** : 63-67, 2001.
18) 長田賢一：急性期躁病の治療．臨床精神薬理 **2** : 743-753, 2000.
19) 岸本　朗：頻発性気分障害（rapid cycler）の治療．臨床精神医学 **22** : 1117-1127, 1993.
20) Kukopulos A, et al : Rapid cyclers, temperament and antidepressants. Compr. Psychiatry **24** : 249-258, 1983.
21) 池田暁史，他：双極性障害の薬物療法．精神科治療学 **17**（増）：183-190, 2002.
22) Gelenberg AJ, et al : Comparison of standard and low serum levels of lithium for maintenance treatment of bipolar disorder. N Eng J Med **321** : 1489-1493, 1989.
23) Shastry BS, : Bipolar disorder : an update. Neurochem Int **46** : 273-279, 2005.
24) Muller-Oerlinghausen B, et al : The impact of lithium long-term medication on suicidal behavior and mortality of bipolar patients. Arch Suicide Res **9** : 307-319, 2005.
25) Tondo L, et al : Lower suicide risk with long-term lithium treatment in major affective illness: a meta analysis. Acta Psychiatr Scand **104** : 163-172. 2001.
26) Goodwin GM, : Recurrence of mania after lithium withdrawal. implication for the use of lithium in the treatment of bipolar affective disorder. Br J Psychiatry **164** : 149-152, 1994.
27) Bowden CL, et al : A randomized, placebo-controlled 12-month trial of divalproex and lithium in treatment of outpatients with bipolar I disorder. Arch Gen Psychiatry **57** : 481-489, 2000.
28) Solomon DA, et al : A pilot study of lithium carbonate plus divalproex sodium for the continuation and maintenance treatment of patients with bipolar I disorder. J Clin Psychiatry **58** : 95-99, 1997.
29) Denicoff KD, et al : Comparative prophylactic efficacy of lithium, carbamazepine and combination in bipolar disorder. J Clin Psychiatry **58** : 470-478, 1997.
30) Hartong EG, et al : Prophylactic efficacy of lithium versus carbamazepine in treatment-naïve bipolar patients. J Clin Psychiatry **64** : 144-151, 2003.

ELSEVIER

NeuroImage

www.elsevier.com/locate/ynimg
NeuroImage 31 (2006) 745 – 753

Functional network of the basal ganglia and cerebellar motor loops in vivo: Different activation patterns between self-initiated and externally triggered movements

Takayuki Taniwaki,[a,b,*] Akira Okayama,[a] Takashi Yoshiura,[c] Osamu Togao,[c] Yasuhiko Nakamura,[c] Takao Yamasaki,[b] Katsuya Ogata,[b] Hiroshi Shigeto,[a] Yasumasa Ohyagi,[a] Jun-ichi Kira,[a] and Shozo Tobimatsu[b]

[a]*Department of Neurology, Graduate School of Medical Sciences, Kyushu University, Maidashi 3-1-1, Fukuoka 812-8582, Fukuoka, Japan*
[b]*Department of Clinical Neurophysiology, Graduate School of Medical Sciences, Kyushu University, Maidashi 3-1-1, Fukuoka 812-8582, Fukuoka, Japan*
[c]*Department of Clinical Radiology, Graduate School of Medical Sciences, Kyushu University, Maidashi 3-1-1, Fukuoka 812-8582, Fukuoka, Japan*

Received 23 August 2005; revised 4 December 2005; accepted 15 December 2005
Available online 7 February 2006

The basal ganglia and cerebellar loops are known to participate differently in self-initiated (SI) and externally triggered (ET) movements. However, no previous neuroimaging studies have illustrated functional organization of these loops in vivo. Here, we aimed to functionally visualize these loops during motor execution using functional magnetic resonance imaging (fMRI) with structural equation modeling (SEM). Twelve normal subjects (24–29 years old) were scanned while performing five different frequencies of sequential left finger movements using either SI or ET movements. Random effect analysis combined with a parametric approach revealed a significant positive linear dependence of cerebral activation upon movement rate in the right Put, GPi, VL, SMC and SMA during SI tasks. During ET tasks, significant positive linear relationships were found in the right SMC, VPL, left CB and DN, whereas tendency for linear relationships was seen in the right PMv. SEM further showed significant interactions within the right basal ganglia–thalamo–motor loop during SI tasks. In contrast, there were significant interactions within the entire right cerebral hemisphere–left cerebellar loop involving CB, DN, VPL, PMv and SMC during ET tasks. Therefore, our modeling approach enabled identification of different contributions of the motor loops of basal ganglia and cerebellum to SI and ET tasks during motor execution.

Keywords: Basal ganglia; Cerebellum; Motor loop; fMRI; Structural equation modeling; Self-initiated movement; Externally triggered movement

Introduction

The basal ganglia and cerebellum are two important groups of subcortical nuclei that have a significant influence on motor functions. Recent anatomical studies revealed that their connections were organized into discrete circuits or 'loops' that reciprocally interconnected a large and diverse set of cerebral cortical areas between the basal ganglia and cerebellum (Alexander et al., 1990; Middleton and Strick, 2000). The basal ganglia–thalamo–motor (BGTM) loop comprises some cortical motor areas including the SMA, PMv and SMC and several subcortical structures such as the Put, GPi and VL. Put is input stage of the basal ganglia and receives projections from SMA, PMv and SMC. GPi receives input from Put and is considered to output nuclei of the basal ganglia. In turn, VL receives projections from GPi that are back-projected to SMA, PMv and SMC (Alexander et al., 1990; Delong, 1990). In the cerebello–cerebral (CC) loop, motor cortices such as SMC or PMv are target structures of outputs from CB via DN and VPL, while cerebellar inputs originate from these motor cortices via the pontine nucleus (Kelly and Strick, 2003).

From a functional point of view, the basal ganglia should not be viewed in isolation, but along with the connections between brain areas within the loops (Alexander et al., 1990). For example, abnormal functions in patients with Parkinson's disease (PD) may

Abbreviations: Put, putamen; GPi, internal segment of the globus pallidus; VL, ventrolateral nucleus of the thalamus; VPL, ventro–posterior–lateral nucleus of the thalamus; SMA, supplementary motor area; SMC, sensorimotor cortex; PMv, ventral premotor cortex; CB, cerebellar hemisphere (anterior lobe); DN, dentate nucleus of the cerebellum.

* Corresponding author. Department of Neurology, Graduate School of Medical Sciences, Kyushu University, Maidashi 3-1-1, Fukuoka 812-8582, Fukuoka, Japan. Fax: +81 92 642 5352.
E-mail address: t_taniwa@neuro.med.kyushu-u.ac.jp (T. Taniwaki).
Available online on ScienceDirect (www.sciencedirect.com).

1053-8119/$ - see front matter © 2005 Elsevier Inc. All rights reserved.
doi:10.1016/j.neuroimage.2005.12.032

result from abnormal alterations between areas rather than abnormalities within areas (Rowe et al., 2002). The cerebellum should also be acknowledged as a connecting structure owing to its similarities with the basal ganglia. However, little is known about the dynamic functional organization of the two loops in vivo. A combination of functional imaging and structural equation modeling (SEM) enables us to construct functional modeling of the brain. These methods have been used to demonstrate functional organization of a variety of networks in visual processing (Büchel and Friston, 1997; McIntosh et al., 1994), auditory learning (Gonzalez-Lima and McIntosh, 1994), semantic processing (Bullmore et al., 2000; Jennings et al., 1998), language processing (Petersson et al., 2000), associative learning (Büchel et al., 1999), facial expression (Iidaka et al., 2001), memory retrieval (Maguire et al., 2001), working memory (Kondo et al., 2004), bimanual motor coordination (Zhuang et al., 2005) and cortical–basal ganglia (Grafton et al., 1994), but no conclusive results on motor loops of the basal ganglia or cerebellum have been reported.

The basal ganglia and cerebellum appear to participate differently in self-initiated (SI) and externally triggered (ET) movements in primates (Middleton and Strick, 2000; Mushiake et al., 1991; Okano and Tanji, 1987; Romo and Schultz, 1987; Romo et al., 1992; van Donkelaar et al., 1999, 2000). It is anticipated that a comparison between SI and ET tasks could depict characteristic features of motor loops of the basal ganglia or cerebellum. However, only a few imaging studies have reported differential activations of the basal ganglia and cerebellum during SI and ET movements (Cunnington et al., 2002; Menon et al., 1998; Rao et al., 1997). So far, no studies have investigated functions of the cortico–subcortical loops and disclosed roles of basal ganglia and the cerebellum in movement execution.

The basal ganglia and cerebellum likely mediate timing or rhythm of paced finger movements (Ivry et al., 1988; O'Boyle et al., 1996; Pastor et al., 1992). Recently, we demonstrated functional interactions within BGTM loop using fMRI with a parametric approach and SEM, while human subjects performed SI paced finger movements at five different rates (Taniwaki et al., 2003). The present study extended the application of these methods to investigate not only the BGTM loop, but also the CC loop in vivo. Therefore, this study aimed to elucidate physiological roles of the basal ganglia and cerebellum during motor execution. To achieve this, we compared functional network models of SI movements and of ET movements and constructed a functional network to account for correlations between BGTM and CC loops.

Materials and methods

Participants

Twelve healthy volunteers (mean age ± SD, 24.9 ± 1.5 years old; range, 23–29 years old; 9 men and 3 women) participated in the study. All subjects were strongly right-handed as assessed by a modified version of the Edinburgh handedness inventory (Oldfield, 1971). All subjects gave an informed written consent. The local ethical committee of Kyushu University approved this study.

Experimental design

The activation paradigm consisted of sequential movements performed with the left hand as previously described (Taniwaki et al., 2003) because non-dominant hand movements caused a greater recruitment of the striatum (Mattay et al., 1998) and cerebellum (Jancke et al., 1999). Subjects were instructed on how to move each finger with changing movement rates. They were then required to practice the tasks before the scan, until they were able to perform them at constant amplitude without error. They were also instructed to keep their eyes closed during MRI. Subjects had to (1) make finger-to-thumb opposition movements in the order of index, middle, ring and little fingers; (2) open and clench the fist twice; (3) complete finger-to-thumb opposition movements in the opposite order (namely, little, third, middle and index fingers); (4) once again open and clench the fist twice; and (5) repeat the same series of 40-s movements in data acquisition. Each finger-to-thumb opposition movement and pair of opening and clenching fist movements was counted as a single movement. During SI tasks, movement rates were set at very slow (as slow as possible), slow, moderate (comfortable pace), fast and very fast (as fast as possible) speeds. During the practice session, movement rates were approximately 0.5 Hz when very slow and nearly 4.0 Hz when very fast among all the subjects. During ET tasks, movement rates were set at 0.5, 1, 2, 3 or 4 Hz for all subjects. Subjects paced their movements in response to a metronome, which consisted of a clicking sound at precise time intervals and was delivered binaurally to the subjects via air conduction through a pair of 2.5-m-long plastic tubes. During rest conditions, subjects were asked to lie down and listen to the metronome used in the ET session. Movements were performed for 40 s (activation) at a constant rate, followed by 40 s of rest (baseline), and were switched by a voice signal. Movement rate conditions were presented in a pseudorandom order within an imaging series. Consequently, there were a total of five baseline/activation (five different rates) cycles per imaging series. Four consecutive imaging series (two SI and two ET) were conducted per subject. Digital video recording was performed throughout the study for subsequent analysis of finger movements. Two-way analysis of variance (ANOVA) with repeated measures was performed to determine effects of movement rates and tasks.

fMRI methods

Images were acquired on a 1.5 T Magnetom SYMPHONY (Siemens, Enlangen, Germany) whole body MRI system with a circular polarized volume head coil. This machine was equipped with real time fMRI software package provided by the manufacturer with scanner. Initially, a set of localized images was acquired to position the image slice. For each session, 100 EPI multislice data sets were acquired (TE, 50 ms; TR, 4 s, flip angle, 90°; acquisition time for the whole paradigm, 400 s). Each multislice data set contained 32 transverse slices (slice thickness, 3.0 mm; interslice gap, 1.0 mm; matrix, 64 × 64; FOV, 23 cm). All images were analyzed using a SPM 2 Software (Wellcome Department of Cognitive Neurology, London, UK). The first three data sets of each time series were discarded, and the remaining EPI volumes were realigned against the first volume. Real time fMRI for main effect analysis was used to monitor patient's motion during the scan. When a severe head motion was detected, the subject was asked to carefully control head motion in the next scan. Consequently, the first series showed serious motion artifacts (>1 mm along each axis) in five subjects, and two of them showed other motion artifacts in the first series of alternative task. It is assumed that first scans include some learning processes, while

second scans mainly reflect over-learned motor processes. Therefore, data sets (one SI and one ET from each subject) were selected from the second trial of each task. Images were spatially normalized against a standard template and smoothed with a Gaussian kernel with 8-mm full width at half maximum (FWHM). The design matrix was set using the box car reference waveform (40-s epoch). The time series in each voxel was high-pass-filtered (160-s cut-off) and scaled to a grand mean of 100 over voxels and scans within each session.

Activation areas

Statistical analysis was performed at two stages. In the first stage, using a single subject fixed effect model, all movement rates were modeled as a delta function (Friston et al., 1998). Data were modeled using a set of orthogonalized polynomial expansions up to the fourth order (Büchel et al., 1996, 1998). Each term was represented by the interaction between a delta function and the average of movement rates exerted during each epoch. In general, the nth order term was given by rate^n · delta. Resulting covariates were convolved with a canonical synthetic hemodynamic response function and were used in a general linear model (Friston et al., 1995), together with a single covariate representing the mean (constant) term over scans. Parameter estimates for each covariate resulting from the least mean squares fit of the model to the data were calculated, and statistical parametric maps of the t statistic (SPM{t}) resulting from linear contrasts of each covariate (Friston et al., 1995) were generated and stored as separate images for each subject.

In order to create activation maps representing main effects of movement rates (0th order), as well as linear (1st order) and non-linear (2nd, 3rd and 4th order) changes of signals in relation to movement rates, random effect analysis was performed (Friston et al., 1999). Data for the second stage of analysis comprised of pooled parameter estimates for each covariate across all subjects. Contrast images for each subject were entered into a one sample t test for each covariate of interest. The SPM{t}s were thresholded at $P < 0.001$ and were uncorrected. Anatomical labels for coordinates in SPM2 (MNI brain template) were defined by Talairach Daemon (http://www.ric.uthscsa.edu/projects/talairachdaemon.html) after a non-linear transform of MNI brain template to Talairach atlas (http://www.mrc-cbu.cam.ac.uk/Imaging/Common/mnispace.shtml). For SEM, ROIs were selected at the local maxima from 1st order linear effect. We investigated the right Put (28, −6, 0), GPi (10, −2, −2), VL (16, −14, 16), VPL (18, −22, 6), SMA (6, −2, 40), SMC (48, −20, 52), DN (18, −54, −22), CB (26, −56, −26), and left VL (−12, −12, 12), VPL (−12, −20, 8), SMA (−6, 0, 42), SMC (−40, −18, 58), DN (−22, −50, −22), CB (−30, −54, −22). For regions without any significant linear relationships at a threshold of $P < 0.001$, the following coordinates were found at the threshold of $P < 0.01$: left Put (−26, −14, 4), GPi (−12, 0, 0), PMv (−56, 0, 32) and right PMv (52, 2, 38).

Structural equation modeling

In this analysis, variables were considered in terms of the covariance structure, with parameters (interregional connection) being estimated by minimizing differences between observed covariance and those implied by a predicted model. The model consisted of anatomically separable regions, and connections were specified between those regions and their directions. Anatomical regions comprised Put, GPi, VL, VPL, SMA, SMC, PMv, CB and DN (Table 1). Connections between brain regions are based on the neuroanatomical knowledge of BGTM and CC loops (Alexander et al., 1990; Delong, 1990; Kelly and Strick, 2003) as described in the Introduction section. Between the two loops, SMA and PMv have reciprocal interconnections with each other and project to SMC (Barbas and Pandya, 1987; Johnson et al., 1996; Muakkassa and Strick, 1979; Rizzolatti et al., 1998; Rowe et al., 2002). Recursive connections from the cortex back to the thalamus have also been documented in such a model (Delong, 1990; Grafton et al.,

Table 1
Parametric analysis of rate-dependent BOLD effects

	Main effect				Linear effect				Polynomial 2			
	Coordinates				Coordinates				Coordinates			
	Z	(x	y	z)	Z	(x	y	z)	Z	(x	y	z)
SI movement												
rPut	5.25	30	−12	−2	4.03	28	−6	0	n.s.			
rGPi	2.08	18	−6	−4	3.29	10	−2	−2	n.s.			
rVL	4.48	10	−16	8	3.41	16	−14	16	n.s.			
rVPL	4.54	14	−20	6	5.12	18	−22	6	n.s.			
rSMA	4.42	4	0	50	3.86	6	−2	40	n.s.			
rSMC	6.09	36	−20	60	4.28	48	−20	52	n.s.			
rPMv	4.23	54	6	34	n.s.				n.s.			
lCB	5.49	−28	−50	−28	n.s.				n.s.			
lDN	4.99	−14	−56	−22	n.s.				n.s.			
lPut	n.s.				2.69	−26	−14	4	n.s.			
lGPi	n.s.				2.94	−12	0	0	n.s.			
lVL	3.97	−16	−8	12	n.s.				n.s.			
lVPL	4.21	−14	−16	6	3.24	−12	−20	8	n.s.			
lSMA	5.39	−2	−2	54	3.34	−6	0	42	n.s.			
lSMC	4.49	−64	−18	34	4.29	−40	−18	58	n.s.			
lPMv	4.53	−58	4	38	2.73	−56	0	32	n.s.			
rCB	4.25	26	−56	−26	4.08	26	−56	−26	n.s.			
rDN	4.21	22	−62	−24	4.48	18	−54	−22	n.s.			
ET movement												
rPUT	3.91	30	−10	−2	n.s.				n.s.			
rGPi	3.08	18	−6	−2	n.s.				n.s.			
rVL	3.83	12	−18	0	n.s.				3.10	16	−8	12
rVPL	3.25	12	−22	8	3.44	16	−22	12	n.s.			
rSMA	4.21	2	−2	54	n.s.				n.s.			
rSMC	5.19	34	−14	56	3.82	46	−18	54	n.s.			
rPMv	3.58	54	2	34	2.99	52	2	38	n.s.			
lCB	5.44	−32	−44	−30	3.94	−30	−54	−22	n.s.			
lDN	5.23	−20	−54	−22	3.92	−22	−50	−22	n.s.			
lPut	n.s.				n.s.				n.s.			
lPGi	n.s.				n.s.				n.s.			
lVL	3.83	−18	−12	18	2.98	−12	−12	12	n.s.			
lVPL	3.09	−14	−18	6	n.s.				n.s.			
lSMA	3.40	−6	−2	44	n.s.				n.s.			
lSMC	3.49	−64	−20	38	n.s.				n.s.			
lPMv	3.83	−56	−4	36	n.s.				n.s.			
rCB	3.29	26	−66	−24	n.s.				n.s.			
rDN	4.13	22	−52	−22	n.s.				n.s.			

Z values refer to activation maximum within the respective region, $P < 0.001$ uncorrected, height threshold $Z > 3.09$ or $P < 0.01$ uncorrected, $Z > 2.33$ in linear effect: SPM coordinates in parenthesis; n.s. = activation below height threshold, Put = putamen, GPi = internal segment of globus pallidus, VL = ventrolateral nucleus of thalamus, VPL = ventro–posterior–lateral nucleus of thalamus, SMA = supplementary motor area, SMC = sensorimotor cortex, PMv = ventral premotor cortex, CB = anterior lobe of the cerebellar hemisphere, DN = dentate nucleus of the cerebellum, r = right, l = left.

1994). Since significant linear effects were observed in bilateral hemispheres, it was decided to construct an anatomical network for bilateral loops. Interhemispheric connections were constructed from a primate study within motor cortices (Rouiller et al., 1994).

fMRI signal changes were calculated using a single subject fixed effect model. Averaged signal changes of baseline epochs were subtracted from those of each task condition, although the first images within each task epoch were excluded to discount the hemodynamic response lag. fMRI data of local maxima in each ROI were standardized to zero mean and to unit variance for each participant (Bullmore et al., 2000; Kondo et al., 2004). Then, individual time series for each location were concatenated into a group matrix for path analysis and subsequent group comparisons (n = 1056) to obtain stable SEM model solutions. Interregional correlations of activity between selected regions were computed and combined with a neuroanatomical model (Fig. 2) to compute structural equation models using LISREL 8.5 (Scientific Software International, Inc., Lincolnwood, IL). A maximum likelihood algorithm was used to fit the parameters. Within-hemisphere functional networks were constructed at first, and a functional network accounting for interhemispheric interactions was calculated in the final stage (McIntosh et al., 1994). The influence of other connections could be estimated by modification indices (McIntosh and Gonzalez-Lima, 1994; McIntosh et al., 1994). Residual influences were set to 0.30 for all regions. Statistical inferences from group differences were based on a stacked model approach including an omnibus test. This procedure determined the χ^2 goodness-of-fit statistic for both a null model, in which path coefficients are equally constrained between conditions, and an alternative model, in which coefficients are allowed to differ (McIntosh et al., 1994). Significance of differences between the models was expressed as the difference in the χ^2 statistic with degrees of freedom equal to differences in degrees of freedom for the null model and alternative model (McIntosh et al., 1994).

Results

Performance of subjects

In general, all subjects showed fairly good performance for SI movements. Very slow movements were performed at a frequency of 0.69 ± 0.16 Hz (mean ± SD), slow movements were performed at 1.00 ± 0.25 Hz, moderate movements were performed at 1.84 ± 0.58 Hz, fast movements were performed at 2.95 ± 0.78 Hz and very fast movements were performed at 4.03 ± 0.94 Hz. ET movement rates were almost identical to rates of auditory triggers (0.5 Hz trigger, 0.51 ± 0.02 Hz; 1 Hz trigger, 1.00 ± 0.01 Hz; 2 Hz trigger, 1.99 ± 0.02 Hz; 3 Hz trigger, 3.01 ± 0.07 Hz; 4 Hz trigger; 3.97 ± 0.07 Hz). Rates of SI and ET movements were very similar without statistically significant differences (P = 0.598, two-way ANOVA with repeated measures).

Foci of activation

To separate regional activities within the same task but at different rate-response functions, a parametric approach based on orthogonal basic functions up to the fourth order was used. In the study of main effects, both tasks caused significant activation at the right posterior Put, bilateral VL, VPL, SMA, SMC, PMv, DN and CB (Table 1; Figs. 1A and B). Significant activation was also seen in the right GP during SI tasks.

A significant positive linear increase in BOLD response magnitude in parallel with finger movement rate emerged at the right Put, GP, VL, DN, CB, bilateral VPL, SMA and SMC during the SI tasks. In ET tasks, a significant positive linear increase occurred in the right VPL, SMC, left VL, CB and DN, and tendency for linear increase was seen in the right PMv (Table 1; Figs. 1C and D). No significant negative linear correlation in terms of a decline in BOLD response in parallel with tapping rate was documented in BGTM or CC loops. A significant non-linear rate-response function (2nd order) was observed in the right VL during ET tasks.

Structural equation modeling

During SI tasks, a significant positive correlation between movement rate and fMRI signal change was found within the BGTM loop, whereas a positive correlation was observed within the CC loop during ET movements. Thus, the BGTM loop appeared to play an important role in rate-dependent motor processing during SI movements, while the CC loop mainly worked during ET tasks. To confirm this hypothesis, functional network analysis was performed within loops. No additional connection improved the fit of the model on modification indices.

Structural equation models of right BGTM and CC

Functional networks for the right hemisphere significantly differed between the two conditions according to the omnibus test [χ^2 diff (29) = 291.21, $P < 0.001$]. BGTM interactions from SMA to right SMC via right Put, right GPi and right VL were stronger during SI tasks. In contrast, entire CC interactions from left CB to left CB via left DN, right VPL, right PMv and right SMC were stronger during ET tasks. As a whole, interactions along the BGTM loop were stronger during SI finger movements, while interactions along the CC loop were stronger during ET finger movements, as predicted by mapping and correlation analyses (Table 2; Fig. 2).

Structural equation models of left BGTM and CC (Table 2; Fig. 2)

The omnibus test suggested that the model in ET task was different from the model in SI [χ^2 diff (29) = 50.28, $P < 0.001$]. Moderate interactions were seen from right CB to right DN during both tasks, which were relatively stronger in SI tasks. Similarly, interactions from left GP to left VL were relatively stronger in SI tasks.

Interhemisphere structural equation models (Table 2; Fig. 2)

The omnibus test indicated that the model in ET task was different from the model in SI [χ^2 diff (12) = 22.63, $P < 0.05$]. Interaction from right PMv to left SMC tended to be stronger in ET task.

Discussion

In the current study, we attempted to elucidate functional interactions within BGTM and CC loops using fMRI with a parametric approach and SEM during sequential finger movements

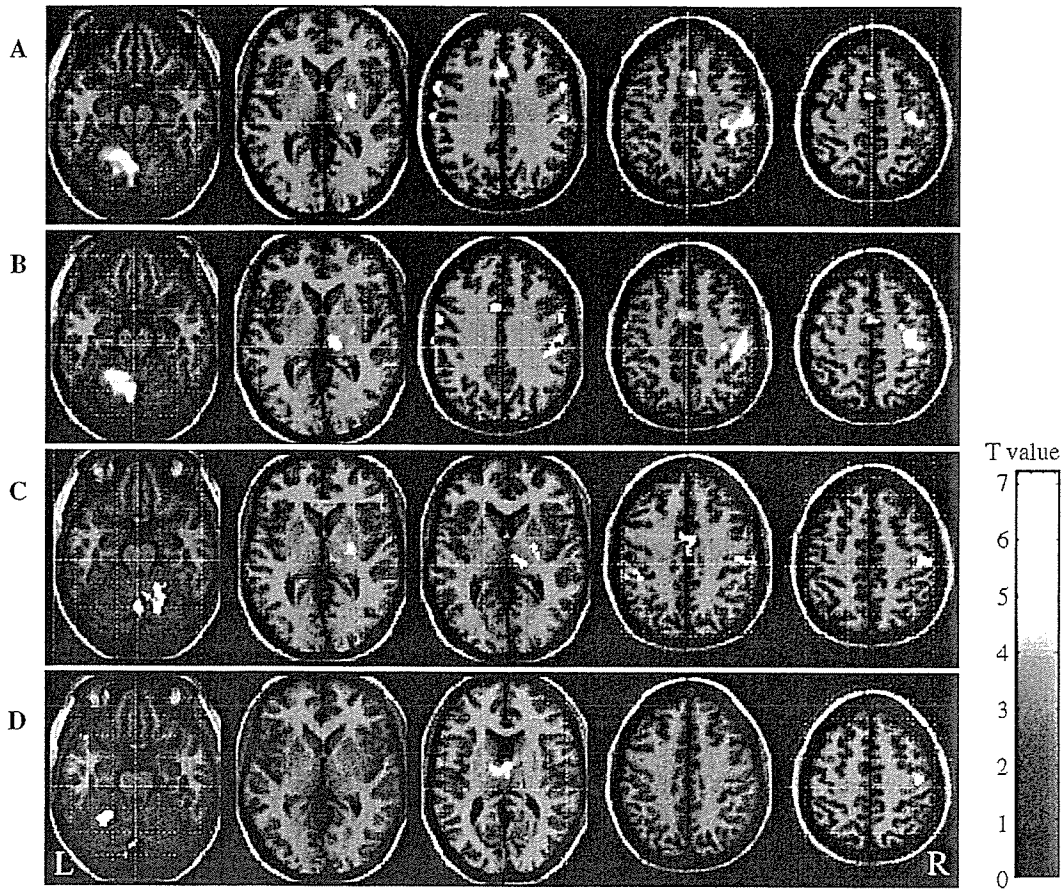

Fig. 1. Regions showing main effects of movement rate (A and B) and significant linear (1st order) relationship between BOLD signal and increasing movement rate (C and D). All regions are significant with $P < 0.001$, uncorrected. (A and C) Self-initiated movements. (B and D) Externally triggered movements. R = right, L = left.

of SI and ET tasks. The major new findings were as follows: (1) maps representing linear changes of signals in relation to movement rate showed significant activations in the BGTM loop during SI movements as well as in the CC loop during ET movements; (2) SEM further confirmed significant interactions in the BGTM loop during SI movements as well as in the CC loop during ET movements.

SI versus ET movements

Patients with PD have difficulties especially in SI or volitional movements (Benecke et al., 1987). A potentially powerful method to separately study BGTM and CC loops is to investigate the differences between SI and ET movements. Previous imaging studies have examined cerebral activation during index finger extensions or arm movements that involved SI or ET movements in neurologically normal subjects and showed no significant differences (Jahanshahi et al., 1995; Jenkins et al., 2000). Activation of the lentiform nucleus was found only during SI movements by an event-related fMRI study (Cunnington et al., 2002). Although activation was bilateral, it was mostly observed on the ipsilateral side, and this study did not show clear activation of the motor loop. Consistent with these results (Jahanshahi et al., 1995; Jenkins et al., 2000; Cunnington et al., 2002), our main effect analysis also showed activation of the same brain regions during SI and ET movement. However, it is interesting to note that our statistical mapping revealed positive dependence of cerebral activation upon movement rate in the right Put, GPi, VL, SMC and SMA during SI tasks. A significant positive linear relationship was found in the right SMC, VPL, left DN, CB and tendency was observed in the right PMv during ET tasks. These results suggest significant activations in the BGTM loop during SI movements as well as in the CC loop during the ET movements. We confirmed these by constructing a loop model and performing a network analysis. SEM has provided new insights into task-specific functional networks (Grafton et al., 1994; McIntosh and Gonzalez-Lima, 1994; McIntosh et al., 1994). In addition, we used correlation data based on rate-dependent movements. This approach provided additional information about brain physiology such as rhythm formation, motor preparation or motor execution that is not always apparent in results of categorical comparisons of fMRI data. Thus, we investigated interactions among the BGTM loop and the CC loop using SEM and constructed a model as shown in Fig. 2.

Our SEM depended on movement rate, and we showed that different systems operated during the two tasks. Most of differences between the two tasks involved interactions within the right supratentorial and left infratentorial lesions. Functional networks for SI movements showed continuous positive interaction from SMA to SMC via Put, GPi and VL. In ET tasks, apparent positive interactions were found in entire CC loops. For the first time, the paths were shown to represent significant roles of the BGTM loop in SI movements as well as the CC loop in ET movements in

Table 2
Path coefficients during two different tasks

	rPut	rGP	rVL	rVPL	rSMA	rSMC	rPMv	lDN	lCB	lPut	lGP	lVL	lVPL	lSMA	lSMC	lPMv	rDN	rCB
SI																		
rPut	–	–	–	–	0.22	0.04	0.11	–	–	–	–	–	–	–	–	–	–	–
rGP	0.54	–	–	–	–	–	–	–	–	–	–	–	–	–	–	–	–	–
rVL	–	0.22	–	–	0.05	0.18	0.12	–	–	–	–	–	–	–	–	–	–	–
rVPL	–	–	–	–	–	0.02	0.04	0.19	–	–	–	–	–	–	–	–	–	–
rSMA	–	–	0.10	–	–	–	−0.01	–	–	–	–	–	–	–	–	0.11	–	–
rSMC	–	–	0.20	0.05	−0.01	–	0.10	–	–	–	–	–	–	0.01	0.14	0.00	–	–
rPMv	–	–	0.14	−0.01	−0.01	–	–	–	–	–	–	–	–	0.05	–	−0.06	–	–
lDN	–	–	–	–	–	–	–	–	0.13	–	–	–	–	–	–	–	–	–
lCB	–	–	–	–	–	0.19	−0.06	–	–	–	–	–	–	–	–	–	–	–
lPut	–	–	–	–	–	–	–	–	–	–	–	–	–	0.11	−0.04	0.05	–	–
lGP	–	–	–	–	–	–	–	–	–	0.17	–	–	–	–	–	–	–	–
lVL	–	–	–	–	–	–	–	–	–	–	0.20	–	–	0.12	0.12	−0.06	–	–
lVPL	–	–	–	–	–	–	–	–	–	–	–	–	–	–	0.08	−0.06	0.07	–
lSMA	–	–	–	–	–	–	0.04	–	–	–	–	0.12	–	–	–	0.09	–	–
lSMC	–	–	–	–	0.16	0.13	0.00	–	–	–	–	0.14	−0.02	−0.02	–	0.15	–	–
lPMv	–	–	–	–	0.11	–	−0.05	–	–	–	–	−0.08	0.09	0.09	–	–	–	–
rDN	–	–	–	–	–	–	–	–	–	–	–	–	–	–	–	–	–	0.41
rCB	–	–	–	–	–	–	–	–	–	–	–	–	–	–	0.09	0.00	–	–
ET																		
rPut	–	–	–	–	−0.05	0.06	0.16	–	–	–	–	–	–	–	–	–	–	–
rGP	0.18	–	–	–	–	–	–	–	–	–	–	–	–	–	–	–	–	–
rVL	–	0.28	–	–	0.08	0.06	0.02	–	–	–	–	–	–	–	–	–	–	–
rVPL	–	–	–	–	–	0.02	−0.04	0.22	–	–	–	–	–	–	–	–	–	–
rSMA	–	–	0.14	–	–	–	0.10	–	–	–	–	–	–	–	–	0.01	–	–
rSMC	–	–	0.08	−0.03	0.18	–	0.20	–	–	–	–	–	–	0.09	0.12	−0.03	–	–
rPMv	–	–	−0.12	0.28	0.10	–	–	–	–	–	–	–	–	0.04	–	0.08	–	–
lDN	–	–	–	–	–	–	–	–	0.26	–	–	–	–	–	–	–	–	–
lCB	–	–	–	–	–	0.28	−0.01	–	–	–	–	–	–	–	–	–	–	–
lPut	–	–	–	–	–	–	–	–	–	–	–	–	–	0.04	−0.02	0.11	–	–
lGP	–	–	–	–	–	–	–	–	–	0.13	–	–	–	–	–	–	–	–
lVL	–	–	–	–	–	–	–	–	–	–	0.14	–	–	0.09	0.03	0.01	–	–
lVPL	–	–	–	–	–	–	–	–	–	–	–	–	–	–	−0.05	0.00	0.12	–
lSMA	–	–	–	–	–	–	0.06	–	–	–	–	0.12	–	–	–	0.11	–	–
lSMC	–	–	–	–	0.05	0.07	0.15	–	–	–	–	−0.07	0.13	0.10	–	0.08	–	–
lPMv	–	–	–	–	0.00	–	0.09	–	–	–	–	−0.02	0.05	0.11	–	–	–	–
rDN	–	–	–	–	–	–	–	–	–	–	–	–	–	–	–	–	–	0.32
rCB	–	–	–	–	–	–	–	–	–	–	–	–	–	–	0.09	0.01	–	–

Abbreviations of regions are the same as in Table 1.

human. These results were consistent with primate studies (van Donkelaar et al., 1999; 2000; Mushiake et al., 1991; Okano and Tanji, 1987; Romo et al., 1992) and, in part, with our previous mapping results (Taniwaki et al., 2003).

SEM results need to be interpreted carefully because of the methodological limitations of SEM. We cannot always interpret a positive path coefficient as an excitatory influence and a negative path coefficient as inhibitory (McIntosh and Gonzalez-Lima, 1994). Instead, positive and negative path coefficients measure signs of covariance relationships among structures of the network. Our current results showed significantly different path coefficients with absolute magnitude between SI and ET tasks. Thus, we can only regard them as quantitative changes within functional network.

Timing of movements

Our experimental tasks depended on movement rate, therefore, our current results might represent neural systems underlying timing of movements or rhythm which is related to structures according to event occurrences. Some human studies suggested that timing was controlled by the lateral cerebellum and the dentate (Casini and Ivry, 1999; Ivry et al., 1988). Patients with PD also demonstrated abnormal timing of paced finger tapping tasks (O'Boyle et al., 1996; Pastor et al., 1992), and dopaminergic treatment improved both motor timing (O'Boyle et al., 1996; Pastor et al., 1992, 2004) and time perception (Malapani et al., 1998). Pathological changes in PD include a loss of nigral dopaminergic neurons projecting to the dorsal putamen (Brooks et al., 1990) whose major output involves SMA (Alexander et al., 1986). Therefore, clinical studies suggested that timing may be mediated by the lateral cerebellum, the putamen and/or SMA.

Our current study showed that BGTM interactions from SMA to SMC via Put, GPi and VL were stronger in the SI tasks. There is a body of convergent data in neuroimaging suggesting critical roles of a medial premotor pathway (SMA and basal ganglia) in the internal representation of time. For example, a previous fMRI study on timing of finger tapping showed that Put, thalamus and SMA were mainly involved in explicit timing

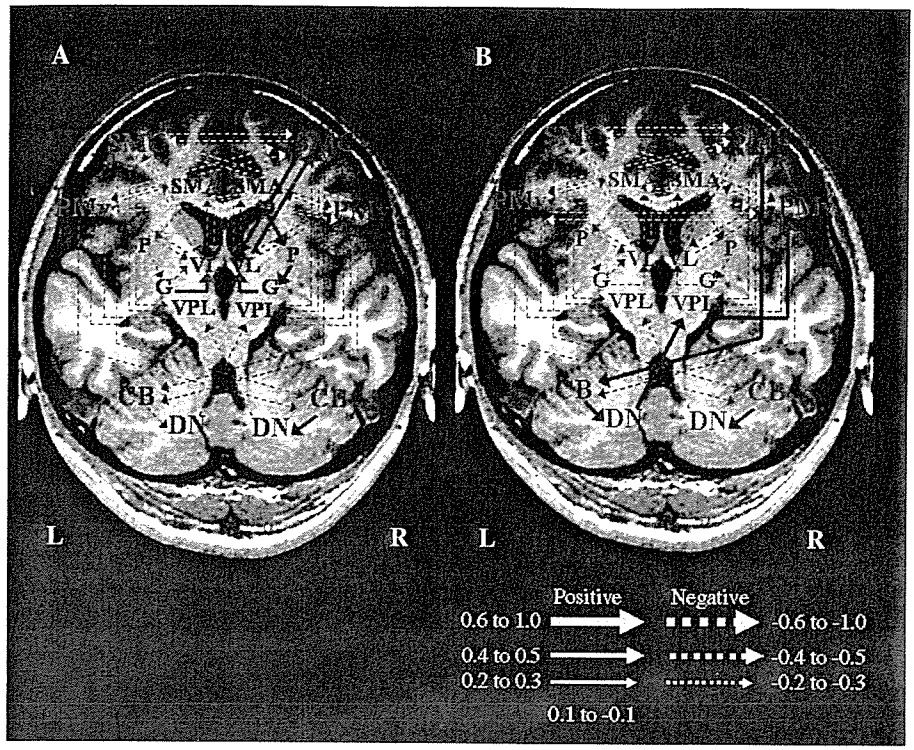

Fig. 2. For graphic representation, significant interactions between the right hemisphere and left cerebellum are shown in red color while those between the left hemisphere and right cerebellum are in blue color for self-initiated (A) and externally triggered movements (B). Interhemispheric functional networks are outlined in yellow color. Positive coefficients (solid arrows) indicate interactions in which an increase of activity in one area is associated with an increase of activity in the other area. Negative coefficients (broken arrows) indicate opposite interactions. P, putamen; G, internal segment of the globus pallidus; VL, ventrolateral nucleus of the thalamus; VPL, ventro–posterior–lateral nucleus and X area of the thalamus; SMA, supplementary motor area; SMC, primary sensory–motor cortex; PMv, ventral premotor cortex; CB, cerebellar hemisphere (anterior lobe); DN, dentate nucleus of the cerebellum.

(Rao et al., 1997). Many neuroimaging studies attempted to dissect the contribution of different timing components (e.g., clock, memory and decision stages) (Gibbon et al., 1984) using time perception tasks and revealed the association of the striatum with encoding time intervals (Harrington et al., 2004; Rao et al., 2001). Not only the basal ganglia but also SMA could be involved in the clock mechanism, as reported in an imaging study on duration perception (Ferrandez et al., 2003). Although our blocked trial design was limited in distinguishing roles of each timing process from sensorimotor or other processes, stronger BGTM interactions in SI tasks might represent central timing processes (SMA, basal ganglia and VL) and sensorimotor processes (SMC).

We also found that entire CC interactions from left CB to left CB via left DN, right VPL, right PMv and right SMC were stronger during ET tasks. Our ET tasks were synchronized coordination (on the beat coordination) (Jantzen et al., 2004; Mayville et al., 2002; Rao et al., 1997), which are quite easy and, once begun, may be carried out with little apparent attentional demand. Previous fMRI studies on simple motor movements under synchronization showed significant activations in the contralateral SMC and ipsilateral cerebellum compared with baseline conditions (Jantzen et al., 2004; Mayville et al., 2002; Rao et al., 1997). Comparisons between synchronization and continuation (off the beat coordination) suggested that CB and SMC were involved in sensorimotor processing rather than explicit timing (Rao et al., 1997). Rao et al. (2001) also suggested involvement of cerebellum in processes other than explicit timing using time perception tasks and event-related fMRI. Other imaging series reported that both synchronization and syncopation required activation of the contralateral SMC and ipsilateral CB, indicating the possibility of monitoring roles of the cerebellum by determining whether movements coincided with the metronome beat or not (Jantzen et al., 2004; Mayville et al., 2002). Thus, stronger CC interactions in our ET tasks indicated not only roles of the cerebellum in monitoring and adjusting inputs from SMC, but also motor planning process in PM and execution process in SMC (Rao et al., 1993; Roland et al., 1980; Samuel et al., 1998).

Functional roles of the contralateral loop

We found moderate interactions from right CB to right DN during both tasks and stronger interaction from left GP to left VL in SI tasks. In several fMRI studies using unilateral finger movements, bilateral activation in the cerebellum was observed during sequential finger movement tasks (Cui et al., 2000; Haaland et al., 2004) or memory-timed finger movements (Kawashima et al., 2000). These results indicate that additional task demand of the complex sequential finger movements may recruit additional regions as a compensatory response. However, SEM showed only partial activation of the contralateral CC loop or BGTM loop, suggesting less involvement of the entire contralateral loops in motor execution.

Concluding remarks

Combined use of sequential finger movements, fMRI and SEM enabled us to visualize functional networks of motor loops in the basal ganglia and cerebellum during motor execution. Different contributions of the two loops to SI and ET tasks were demonstrated. This approach also showed interhemispheric interactions between motor cortices. Our SEM modeling was compatible with findings of non-primate electrophysiological studies. Although there are some limitations of interpretation, it is possible to accomplish in vivo neuroimaging for neurological disorders in which different contributions of the BGTM or CC loops are established in neuropathology.

References

Alexander, G.E., Delong, M.R., Strick, P.L., 1986. Parallel organization of functionally segregated circuits linking basal ganglia and cortex. Annu. Rev. Neurosci. 9, 357–381.

Alexander, G.E., Crutcher, M.D., Delong, M.R., 1990. Basal ganglia thalamo–cortical circuits: parallel substrates for motor, oculomotor, "prefrontal" and "limbic" functions. Prog. Brain Res. 85, 119–146.

Barbas, H., Pandya, D.N., 1987. Architecture and frontal cortical connections of the premotor cortex (area 6) in the rhesus monkey. J. Comp. Neurol. 256, 211–228.

Benecke, R., Rothwell, J.C., Dick, J.P.R., Day, B.L., Marsden, C.D., 1987. Disturbance of sequential movements in patients with Parkinson's disease. Brain 110, 361–379.

Brooks, D.J., Ibanez, V., Sawle, G.V., Quinn, N., Lees, A.J., Mathias, C.J., Bannister, R., Marsden, C.D., Frackowiak, R.S., 1990. Differing patterns of striatal 18F-dopa uptake in Parkinson's disease, multiple system atrophy and progressive supranuclear palsy. Ann. Neurol. 28, 547–555.

Büchel, C., Friston, K.J., 1997. Modulation of connectivity in visual pathways by attention: cortical interactions evaluated with structural equation modeling and fMRI. Cereb. Cortex 7, 768–778.

Büchel, C., Wise, R.J.S., Mummery, C.J., Poline, J.-B., Friston, K.J., 1996. Nonlinear regression in parametric activation studies. NeuroImage 4, 60–66.

Büchel, C., Holmes, A.P., Rees, G., Friston, K.J., 1998. Characterizing stimulus–response functions using nonlinear regressors in parametric fMRI experiments. NeuroImage 8, 140–148.

Büchel, C., Coull, J.T., Friston, K.J., 1999. The predictive value of changes in effective connectivity for human learning. Science 283, 1538–1541.

Bullmore, E., Horwitz, B., Honey, G., Brammer, M., Williams, S., Sharma, T., 2000. How good is good enough in path analysis of fMRI data? NeuroImage 11, 289–301.

Casini, L., Ivry, R.B., 1999. Effects of divided attention on temporal processing in patients with lesions of the cerebellum or frontal lobe. Neuropsychology 13, 10–21.

Cui, S.Z., Li, E.Z., Zang, Y.F., Weng, X.C., Ivry, R., Wang, J.J., 2000. Both sides of human cerebellum involved in preparation and execution of sequential movements. NeuroReport 11, 3849–3853.

Cunnington, R., Windischberger, C., Deecke, L., Moser, E., 2002. The preparation and execution of self-initiated and externally-triggered movement: a study of event-related fMRI. NeuroImage 15, 373–385.

Delong, M.R., 1990. Primate models of movement disorders of basal ganglia origin. Trends. Neurosci. 13, 281–285.

Ferrandez, A.M., Hugueville, L., Lehericy, S., Poline, J.B., Marsault, C., Pouthas, V., 2003. Basal ganglia and supplementary motor area subtend duration perception: an fMRI study. NeuroImage 19, 1532–1544.

Friston, K.J., Holmes, A.P., Worsley, K.J., Poline, J.-P., Frith, C.D., Frackowiak, R.S., 1995. Statistical parametric maps in functional imaging: a general linear approach. Hum. Brain Mapp. 2, 189–210.

Friston, K.J., Fletcher, P., Josephs, O., Holmes, A., Rugg, M.D., Turner, R., 1998. Event-related fMRI: characterizing differential responses. NeuroImage 7, 30–40.

Friston, K.J., Holmes, A.P., Worsley, K.J., 1999. How many subjects constitute a study? NeuroImage 10, 1–5.

Gibbon, J., Church, R.M., Meck, W.H., 1984. Scalar timing in memory. Ann. N. Y. Acad. Sci. 423, 52–77.

Gonzalez-Lima, F., McIntosh, A.R., 1994. Neural network interactions related to auditory learning analyzed with structural equation modeling. Hum. Brain Mapp. 2, 23–44.

Grafton, S.T., Sutton, J., Couldwell, W., Lew, M., Waters, C., 1994. Network analysis of motor system connectivity in Parkinson's disease: modulation of thalamocortical interactions after pallidotomy. Hum. Brain Mapp. 2, 45–55.

Haaland, K.Y., Elsinger, C.L., Mayer, A.R., Durgerian, S., Rao, S.M., 2004. Motor sequence complexity and performing hand produce differential patterns of hemispheric lateralization. J. Cogn. Neurosci. 16, 621–636.

Harrington, D.L., Boyd, L.A., Mayer, A.R., Sheltraw, D.M., Lee, R.R., Huang, M., Rao, S.M., 2004. Neural representation of interval encoding and decision making. Cogn. Brain Res. 21, 193–205.

Iidaka, T., Omori, M., Murata, T., Kosaka, H., Yonekura, Y., Okada, T., Sadato, N., 2001. Neural interaction of the amygdala with the prefrontal and temporal cortices in the processing of facial expressions as revealed by fMRI. J. Cogn. Neurosci. 13, 1035–1047.

Ivry, R.B., Keele, S.W., Diener, H.C., 1988. Dissociation of the lateral and medial cerebellum in movement timing and movement execution. Exp, Brain Res. 73, 167–180.

Jahanshahi, M., Jenkins, I.H., Brown, R.G., Marsden, C.D., Passingham, R.E., Brooks, D.J., 1995. Self-initiated versus externally triggered movements. I. An investigation using measurement of regional cerebral blood flow with PET and movement-related potentials in normal and Parkinson's disease subjects. Brain 118, 913–933.

Jancke, L., Specht, K., Mirzazade, S., Peters, M., 1999. The effect of finger-movement speed of the dominant and subdominant hand on cerebellar activation: a functional magnetic resonance imaging study. NeuroImage 9, 497–507.

Jantzen, K.J., Steinberg, F.L., Kelso, J.A.S., 2004. Brain networks underlying human timing behavior are influences by prior context. Proc. Natl. Acad. Sci. U. S. A. 101, 6815–6820.

Jenkins, I.H., Jahanshahi, M., Jueptner, M., Passingham, R.E., Brooks, D.J., 2000. Self-initiated versus externally triggered movements: II. The effect of movement predictability on regional cerebral blood flow. Brain 123, 1216–1228.

Jennings, J.M., McIntosh, A.R., Kapur, S., 1998. Mapping neural interactivity onto regional activity: an analysis of semantic processing and response mode interactions. NeuroImage 7, 244–254.

Johnson, P.B., Ferraina, S., Bianchi, L., Caminiti, R., 1996. Cortical networks for visual reaching: physiological and anatomical organization of frontal and parietal lobe arm regions. Cereb. Cortex 6, 102–119.

Kawashima, R., Okuda, J., Uematsu, A., Sugiura, M., Inoue, K., Suzuki, K., Tabuchi, M., Tsukiura, T., Narayan, S.L., Yanagawa, I., Fujii, T., Takahashi, S., Fukuda, H., Yamadori, A., 2000. Human cerebellum plays an important role in memory-timed finger movement: an fMRI study. J. Neurophysiol. 83, 1079–1087.

Kelly, R.M., Strick, P.L., 2003. Cerebellar loops with motor cortex and prefrontal cortex of a nonhuman primate. J. Neurosci. 23, 8432–8444.

Kondo, H., Morishita, M., Osaka, N., Osaka, M., Fukuyama, H., Shibasaki, H., 2004. Functional roles of the cingulo-frontal network in performance on working memory. NeuroImage 21, 2–14.

Maguire, E.A., Vargha-Khadem, F., Mishkin, M., 2001. The effects of bilateral hippocampal damage on fMRI regional activations and interactions during memory retrieval. Brain 124, 1156–1170.

Malapani, C., Rakitin, B., Levy, R., Meck, W.H., Deweer, B., Dubois, B., Gibbon, J., 1998. Coupled temporal memories in Parkinson's disease: a dopamine-related dysfunction. J. Cogn. Neurosci. 10, 316–331.

Mattay, V.S., Callicott, J.H., Bertolino, A., Santha, A.K.S., van Horn, J.D., Tallent, K.A., Frank, J.A., Weinberger, D.R., 1998. Hemispheric control

of motor function: a whole brain echo planar fMRI study. Psychiatry Res. 83, 7–22.
Mayville, J.M., Jantzen, K.J., Fuchs, A., Steinberg, F.L., Kelso, J.A.S., 2002. Cortical and subcortical networks underlying syncopated and synchronized coordination revealed using fMRI. Hum. Brain Mapp. 17, 214–229.
McIntosh, A.R., Gonzalez-Lima, F., 1994. Structural equation modeling and its application to network analysis in functional brain imaging. Hum. Brain Mapp. 2, 2–22.
McIntosh, A.R., Grady, C.L., Ungereider, L.G., Haxby, J.V., Rapoport, S.I., Horwitz, B., 1994. Network analysis of cortical visual pathways mapped with PET. J. Neurosci. 14, 655–666.
Menon, V., Glover, G.H., Pfefferbaum, A., 1998. Differential activation of dorsal basal ganglia during externally and self paced sequences of arm movements. NeuroReport 9, 1567–1573.
Middleton, F.A., Strick, P.L., 2000. Basal ganglia and cerebellar loops: motor and cognitive circuits. Brain Res. Rev. 31, 236–250.
Muakkassa, K.F., Strick, P.L., 1979. Frontal lobe inputs to primate motor cortex: evidence for four somatotopically organized 'premotor areas'. Brain Res. 177, 176–182.
Mushiake, H., Inase, M., Tanji, J., 1991. Neuronal activity in the primate premotor, supplementary, and precentral motor cortex during visually guided and internally determined sequential movements. J. Neurophysiol. 66, 705–718.
O'Boyle, D.J., Freeman, J.S., Cody, F.W.J., 1996. The accuracy and precision of timing of self-paced, repetitive movements in subjects with Parkinson's disease. Brain 119, 51–70.
Okano, K., Tanji, J., 1987. Neuronal activities in the primate motor fields of the agranular frontal cortex preceding visually triggered and self-paced movement. Exp. Brain Res. 66, 155–166.
Oldfield, R.C., 1971. The assessment and analysis of handedness: the Edinburgh inventory. Neuropsychologia 9, 97–113.
Pastor, M.A., Artieda, J., Jahanshahi, M., Obeso, J.A., 1992. Performance of repetitive wrist movements in Parkinson's disease. Brain 115, 875–891.
Pastor, M.A., Day, B.L., Macaluso, E., Friston, K.J., Frackowiak, R.S.J., 2004. The functional neuroanatomy of temporal discrimination. J. Neurosci. 24, 2585–2591.
Petersson, K.M., Reis, A., Askelof, S., Castro-Caldas, A., Ingvar, M., 2000. Language processing modulated by literacy: a network analysis of verbal repetition in literate and illiterate subjects. J. Cogn. Neurosci. 12, 364–382.
Rao, S.M., Binder, J.R., Bandettini, P.A., Hammeke, T.A., Yetkin, F.Z., Jesmanowicz, A., Lisk, L.M., Morris, G.L., Mueller, W.M., Estkowski, L.D., et al., 1993. Functional magnetic resonance imaging of complex human movements. Neurology 43, 2311–2318.
Rao, S.M., Harrington, D.L., Haaland, K.Y., Bobholz, J.A., Cox, R.W., Binder, J.R., 1997. Distributed neural systems underlying the timing of movements. J. Neurosci. 17, 5528–5535.
Rao, S.M., Mayer, A.R., Harrington, D.L., 2001. The temporal evolution of brain activation during temporal processing. Nat. Neurosci. 4, 317–323.
Rizzolatti, G., Luppino, G., Matelli, M., 1998. The organization of the cortical motor system: new concepts. Electroencephalogr. Clin. Neurophysiol. 106, 283–296.
Roland, P., Larsen, B., Lassen, N., Skinhoj, E., 1980. Supplementary motor area and other cortical areas in organization of voluntary movements in man. J. Neurophysiol. 43, 118–136.
Romo, R., Schultz, W., 1987. Neuronal activity preceding self-initiated or externally timed arm movements in area 6 of monkey cortex. Exp. Brain Res. 67, 656–662.
Romo, R., Scarnati, E., Schultz, W., 1992. Role of primate basal ganglia and frontal cortex in the internal generation of movements: II. Movement-related activity in the anterior striatum. Exp. Brain Res. 91, 385–395.
Rouiller, E.M., Babalian, A., Kazennikov, O., Moret, V., Yu, X.M., Wiesendanger, M., 1994. Transcallosal connections of the distal forelimb representations of the primary and supplementary motor cortical areas in macaque monkeys. Exp. Brain Res. 102, 227–243.
Rowe, J., Stephan, K.E., Friston, K., Frackowiak, R.S., Lees, A., Passingham, R., 2002. Attention to action in Parkinson's disease: impaired effective connectivity among frontal cortical regions. Brain 125, 276–289.
Samuel, M., Williams, S., Leigh, P., Simmons, A., Chakraborti, S., Andrew, C., Friston, K., Goldstein, L., Brooks, D.J., 1998. Exploring the temporal nature of hemodynamic responses of cortical motor areas using functional MRI. Neurology 51, 3171–3176.
Taniwaki, T., Okayama, A., Yoshiura, T., Nakamura, Y., Goto, Y., Kira, J., Tobimatsu, S., 2003. Reappraisal of the motor role of basal ganglia: a functional magnetic resonance image study. J. Neurosci. 23, 3432–3438.
van Donkelaar, P., Stein, J.F., Passingham, R.E., Miall, R.C., 1999. Neuronal activity in the primate motor thalamus during visually triggered and internally generated limb movements. J. Neurophysiol. 82, 934–945.
van Donkelaar, P., Stein, J.F., Passingham, R.E., Miall, R.C., 2000. Temporary inactivation in the primate motor thalamus during visually triggered and internally generated limb movements. J. Neurophysiol. 83, 2780–2790.
Zhuang, J., LaConte, S., Peltier, S., Zhang, K., Hu, X., 2005. Connectivity exploration with structural equation modeling: an fMRI study of bimanual motor coordination. NeuroImage 25, 462–470.

ELSEVIER

Clinical Neurophysiology 117 (2006) 2236–2242

www.elsevier.com/locate/clinph

EEG findings in early-stage corticobasal degeneration and progressive supranuclear palsy: A retrospective study and literature review

Kenshi Tashiro [a,b,*], Katsuya Ogata [b], Yoshinobu Goto [b], Takayuki Taniwaki [a], Akira Okayama [a], Jun-ichi Kira [a], Shozo Tobimatsu [b]

[a] *Department of Neurology, Neurological Institute, Graduate School of Medical Sciences, Kyushu University, 3-1-1 Maidashi, Higashi-Ku, Fukuoka 812-8582, Japan*

[b] *Department of Clinical Neurophysiology, Neurological Institute, Graduate School of Medical Sciences, Kyushu University, 3-1-1 Maidashi, Higashi-Ku, Fukuoka 812-8582, Japan*

Accepted 11 June 2006
Available online 21 August 2006

Abstract

Objective: Although neuroimaging and electrophysiological tests are potentially useful to distinguish corticobasal degeneration (CBD) from progressive supranuclear palsy (PSP), little is known about the diagnostic value of electroencephalography (EEG) for their distinction. We assessed the value of EEG for differentiating CBD from PSP.

Methods: We reviewed conventional EEGs recorded at an early stage of disease in 10 CBD patients and 14 PSP patients. We focused on slowing of background activity (SBA), frontal intermittent rhythmic delta activity (FIRDA) and focal slow waves (FSWs). Statistical analysis was performed by Fisher's exact test.

Results: SBA was observed in 1 CBD patient and 2 PSP patients. FSWs were found in 8 CBD patients (80.0%), but only 2 PSP patients (14.3%) ($p = 0.002$); they appeared contralateral to the dominantly-affected side in 6 of 8 CBD patients, and ipsilateral to the side with most atrophy on MRI in 7 of 8 CBD patients. FIRDA was observed in 2 CBD patients (20.0%) and 5 PSP patients (35.7%) ($p = 0.357$).

Conclusions: FSWs are characteristic of CBD, but FIRDA was not disease-specific.

Significance: FSWs on EEG, in addition to clinical criteria, yield useful supplementary information to distinguish between these diseases at early stages.

Keywords: Corticobasal degeneration; Progressive supranuclear palsy; Electroencephalography; Focal slow waves; Frontal intermittent rhythmic delta activity; Slowing of the background activity

1. Introduction

Corticobasal degeneration (CBD) is a slowly progressive extrapyramidal disorder characterized by akinesia and rigidity, associated with cortical signs and involuntary movements with remarkable asymmetry (Rebeiz et al., 1968; Gibb et al., 1989; Riley et al., 1990). CBD can be clinically diagnosed while patients are still alive on the basis of cortical signs that include limb apraxia, alien limb syndrome, cortical reflex myoclonus or cortical sensory impairment; however, pathological findings are necessary to make a definitive diagnosis (Rebeiz et al., 1968). The clinical findings of CBD partially resemble those of progressive supranuclear palsy (PSP) (Rinne et al., 1994). In particular, executive disturbances, parkinsonian features and gaze palsy in CBD might cause difficulty in differentiating CBD from PSP by clinical examination (Rinne et al., 1994). Moreover,

* Corresponding author. Tel.: +81 92 642 5543; fax: +81 92 642 5545.
E-mail address: ketashi@neurophy.med.kyushu-u.ac.jp (K. Tashiro).

1388-2457/$32.00
doi:10.1016/j.clinph.2006.06.710

similarities between the pathologies of Pick's disease, frontotemporal dementia, primary progressive aphasia, CBD, and PSP, and the overlap in clinical patterns during the evolution of these diseases, have led to the concept of Pick's complex (Kertesz, 2003).

Neuroimaging or electrophysiological examinations are considered to be potentially useful in the differential diagnosis of CBD and PSP (Eidelberg et al., 1991; Sawle et al., 1991; Nagasawa et al., 1996; Takeda et al., 1998; Taniwaki et al., 1998; Wang et al., 2000). A focal abnormality of conventional electroencephalography (EEG) was reported in some CBD patients (Riley et al., 1990; Vion-Dury et al., 2004), while the diffuse slow abnormalities including frontal intermittent rhythmic delta activity (FIRDA) were observed in PSP patients (Su and Goldensohn, 1973; Fowler and Harrison, 1986; Torbjoern et al., 1989). Although these EEG findings may have potential value for early diagnosis of CBD or PSP, a systematic study using conventional EEG to compare both diseases has not been performed. Therefore, we compared the findings of conventional EEGs in a more representative sample of individuals fulfilling clinical criteria for CBD with those from a group of patients with a clinical diagnosis of PSP, to ascertain whether EEG could be useful in differentiating CBD from PSP.

2. Methods

2.1. Patients

We retrospectively reviewed the medical records of all patients (Table 1). Ten patients with CBD (50–72 years old) and 14 patients with PSP (44–77 years old) were included. All patients were consecutive cases among approximately 25,300 patients at the Department of Neurology, Kyushu University Hospital, which is the main regional and referral center, from January 1985 to May 2000.

Patients with CBD were selected on the basis of the following diagnostic criteria (Riley and Lang, 2000): mandatory inclusion criteria consisted of (1) chronic progressive course at age 40 or later, (2) asymmetric at onset; (3) presence of higher cortical dysfunction (apraxia, cortical sensory loss, or alien limb) and movement disorders (akinetic-rigid syndrome resistant to levodopa, and limb dystonia or spontaneous and reflex focal myoclonus). Exclusion criteria were (1) early vertical gaze palsy, (2) severe autonomic disturbances, (3) lesions on imaging studies indicating another pathologic process is responsible.

The diagnosis of PSP was made on the basis of the NINDS-SPSP clinical criteria (Litvan et al., 1996). Mandatory inclusion criteria consisted of (1) a gradually

Table 1
Clinical and electroencephalographic features of patients with CBD and PSP

Case	No	Age at EEG (years)	Disease duration (months)	Sex	Dominantly-affected limb	Background activity (Hz)	FSWs focus	FIRDA	Other frequencies	Asymmetrical cortical atrophy on MRI	Brainstem atrophy on MRI
CBD	1	68	12	F	L.	8–9	–	+	Diffuse theta	R.H	–
	2	57	10	F	R.	7–8[a]	L.AT	–		L.FP	–
	3	60	24	F	R.	10	L.A	–		L.H	–
	4	72	30	F	L.	8–9	L.A	+	Diffuse theta	L.P	–
	5	63	24	M	R.	9	L.A	–		L.P	–
	6	59	30	F	R.	10	L.AT	–		L.FP	–
	7	69	24	F	R.	9–10	L.T	–		L.P	–
	8	50	36	M	L.	10	R.T	–		R.H	–
	9	69	7	M	R.	9	–	–		–	–
	10	61	9	F	R.	10	B.	–		L.FP	–
PSP	1	71	36	M	–	9	–	–		–[b]	–
	2	44	24	M	–	8–9	–	+		–	+
	3	49	24	F	–	8–11	–	+		–	–
	4	58	48	F	–	8–9	–	+	Diffuse theta	–[b]	–
	5	66	36	F	–	8–9	–	+	Theta at AT	–	–
	6	75	18	F	–	8–10	R.A	–		–	–
	7	62	24	F	–	8–10	L.A	+		–	+
	8	68	18	F	–	10–11	–	–		–	+
	9	70	24	M	–	8[a]	–	–		–	+
	10	68	6	F	–	9–10	–	–		–	+
	11	66	36	F	–	9	–	–		–	+
	12	66	6	M	–	8–9	–	–	Diffuse theta	–	+
	13	77	9	F	–	11	–	–		–	–
	14	68	8	F	–	8[a]	–	–		–	–

FSWs, focal (intermittent) slow waves; FIRDA, frontal intermittent rhythmic delta activity; L., left; R., right; B., bilateral but independent with each other; A, anterior; AT, anterior temporal; F, frontal; FP, frontoparietal; H, hemisphere; P, parietal; T, temporal; +, positive; –, negative.

[a] Indicates the presence of slow background activity.

[b] Represents patients that had CT instead of MRI.

progressive disorder with onset at age 40 or later, (2) vertical supranuclear gaze palsy, (3) prominent postural instability with falls in the first year of onset. Exclusion criteria were (1) encephalitis, (2) alien limb syndrome, cortical sensory deficits, focal frontal or temporoparietal atrophy, (3) hallucination or delusions, (4) cortical dementia of Alzheimer's type, (5) prominent, early cerebellar symptoms or prominent, early unexplained dysautonomia, (6) severe, asymmetric parkinsonian signs, (7) neuroradiologic evidence of relevant structural abnormality.

No patients used centrally active drugs, nor did any have metabolic abnormalities that might influence the EEG findings. Eight CBD patients and all PSP patients were given the revised Wechsler Adult Intelligence Scale (WAIS-R) test. Two PSP patients had head CT, while other PSP patients and all CBD patients had head MRI.

2.2. EEG recordings

Between 1985 and 1994, conventional awake EEGs were recorded in all patients with a 14-channel analogue EEG system with ECG and electrooculogram (EOG); and after 1995, with a 22-channel digital EEG system including EEG, ECG, and EOG (NIHON KOHDEN, Tokyo, Japan). One or two EEGs per patient were recorded and a total of 28 EEGs (14 EEGs in CBD patients and 14 in PSP patients) were reviewed. For all patients the earliest EEG recorded at their first medical examination in our hospital was analyzed. Thus, 10 EEGs in CBD patients and all 14 EEGs in PSP patients were accepted. EEGs were obtained according to the International 10–20 system of scalp electrode placement. Routine records were obtained (TC 0.3 s, HF 60 Hz) at rest, during hyperventilation and bright white flash flicker stimulation. Standard runs of bipolar, as well as the referential derivation, were employed. Two blinded EEG specialists investigated the abnormalities on each record. EEG changes were classified as showing a particular change in background activity – frequency of dominant rhythm, frontal intermittent rhythmic delta activity (FIRDA), and focal slow wave abnormalities (FSWs) with asymmetry. If the frequency of the dominant rhythm was 8 Hz and below, we defined the slowing of background activity (SBA). The criterion of FSWs was delta or theta waves that localized focally

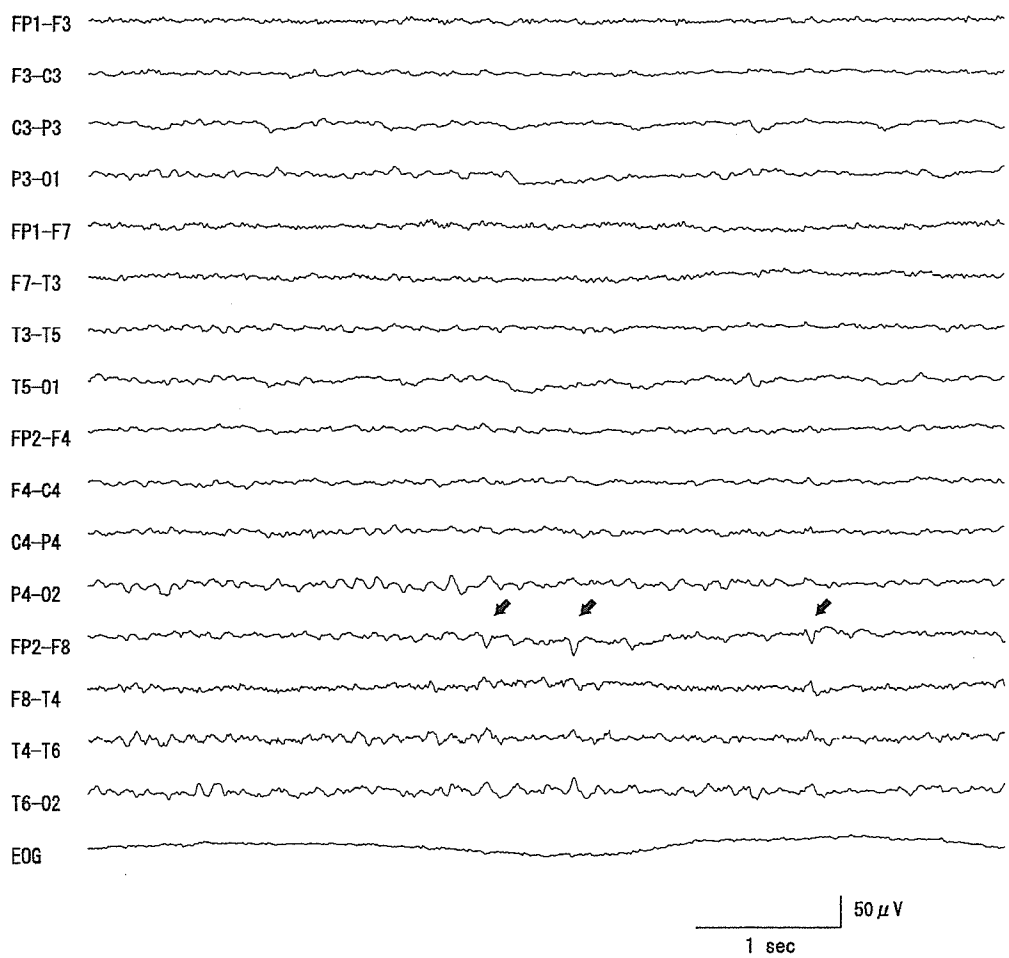

Fig. 1. Representative EEGs in a CBD patient (50-year-old male; case 8). Note that the focal slow wave activities (FSWs) appear in the right anterior temporal area (arrows). MRI revealed brain atrophy on the same side in this patient. EEGs were recorded with a 22-channel digital system.